

ON PULSE-COUPLED DISCRETE-TIME PHASE LOCKED LOOPS FOR WIRELESS NETWORKS

O. Simeone⁽¹⁾, *U. Spagnolini*⁽²⁾ and *Y. Bar-Ness*⁽¹⁾

⁽¹⁾ CWCSR, New Jersey Institute of Technology, Newark, New Jersey 07102-1982, USA

⁽²⁾ DEI, Politecnico di Milano, Milano, I-20133 Italy

E-mail: {osvaldo.simeone, yeheskel.barness}@njit.edu, spagnoli@elet.polimi.it

ABSTRACT

Mutual clock synchronization over a wireless channel has been recently studied in the framework of pulse-coupled oscillators using either models borrowed from mathematical biology or the model of coupled discrete-time Phase Locked Loops (PLLs). In this paper, we focus on the latter case and extend previous analyses by considering frequency-asynchronous clocks, second-order PLLs and by addressing the issues of propagation delays, finite pulse resolution and half-duplex constraints. Moreover, we provide a steady-state and convergence analysis of the system under the ideal assumption of infinite-resolution time error detectors, exploiting some results from the literature on consensus of multi-agents networks. Finally, numerical examples are discussed that corroborate the analysis and show the impact of system parameters such as transmit/receive switching time and oversampling factor at the receiver.

Index Terms— Synchronization, Communication systems, Distributed algorithms.

1. INTRODUCTION

Mutual timing synchronization among nodes of a wireless networks enables an increasingly large number of applications in ad hoc and sensor networks (see, e.g., [1]). Examples range from complex sensing tasks (distributed detection/ estimation, data fusion) to medium access control for communication (e.g., Time Division Multiple Access). Recently, the traditional packet-based approach to mutual synchronization (i.e., nodes exchange packets with appropriate time-stamp [1] [2]) has been challenged by physical layer-based techniques, where local time information is exchanged among distributed clocks through transmission of pulses [3]. The model of pulse-coupled oscillators used in the above mentioned literature is successful in explaining the mutual synchronization of (frequency-synchronous) clocks, but it appears to be hard to generalize and to relate to known results on traditional synchronization systems based on Phase Locked Loops (PLLs).

The goal of this work is to reconsider the problem of mutual clock synchronization through pulse-coupled oscillators by using conventional (discrete-time) linear PLLs. The model can be seen as the discrete-time counterpart of the system of continuously-coupled analog (linearized) PLLs studied in [4]. First-order PLLs for mutual time (phase) synchronization in the presence of frequency-synchronous clocks have been considered in [8] [9] and, recently, in [2], where a

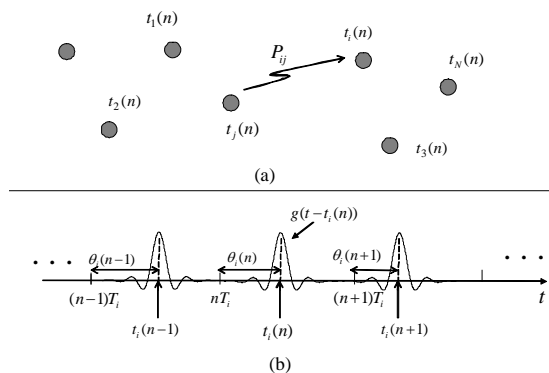


Fig. 1. (a) Network of discrete-time clocks $t_i(n)$ connected through a wireless channel. (b) Illustration of the signal transmitted by the i th node.

convergence proof is provided by leveraging tools from algebraic graph theory. Notice that all these works, with the exception of [9], do not deal with finite-resolution of pulses¹. Finally, the framework of distributed PLLs has strong connections with the literature on consensus of multi-agent networks (see [5] for an overview) and distributed estimation [6]. In fact, a special case of the system considered here (first-order PLLs with frequency-synchronous clocks [8] [9] [2]) coincides with the conventional discrete-time consensus model [5], and a (non-linear) continuous-time model similar to the one studied here is investigated in [6] as a means to achieve global distributed estimation.

The main contributions of this paper are:

1. we introduce the model of pulse-coupled discrete-time PLLs with arbitrary loop order, accounting for finite time-resolution of transmitted pulses and propagation delays;
2. we provide an analysis of steady-state and convergence properties of the system of second-order PLLs under the ideal assumption of infinite-resolution time error detectors: results here exploits tools from algebraic graph theory, similarly to [5], and show that conclusions well known in the context of conventional point-to-point PLLs extend naturally to a distributed system;
3. we corroborate the analysis with numerical results, that illus-

¹Reference [2] assumes in fact packet-based synchronization.

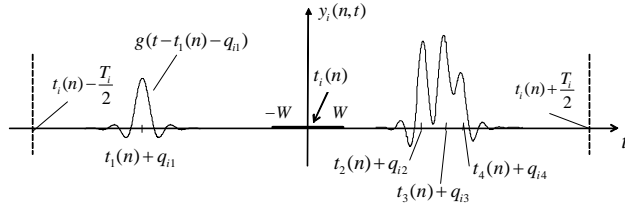


Fig. 2. Sketch of the received signal in the observation window around the "firing" instant $t_i(n)$ (W measure the refractory time due to half-duplex constraint).

trate the impact of finite-resolution, noise and system parameters such as oversampling factor at the receiving side.

2. PULSE-COUPLED SYNCHRONIZATION

We consider a network of N clocks with different free-oscillation frequencies $\{1/T_i\}_{i=1}^N$ arising from random frequency offsets around a nominal value [4]. Nodes communicate over a wireless channel and the topology of the network determines the power P_{ij} received by any i th node from the j th as $P_{ij} = C_{ij}/d_{ij}^\gamma$, where C_{ij} is an appropriate constant (accounting for possible fading and shadowing), $d_{ij} = d_{ji}$ is the distance between the nodes and γ is the path loss exponent ($\gamma = 2 \div 4$) (see fig. 1).

The i th clock is defined by a discrete-time function $t_i(n)$, that, in case of isolated (or uncoupled) nodes, evolves as $t_i(n) = nT_i + \theta_i(0)$, where index $n = 1, 2, \dots$ runs over the periods of the clock and $0 \leq \theta_i(0) < T_i$ is an arbitrary initial phase. Notice that, in order to simplify the analysis, we are neglecting phase noise and frequency drifts [4]. Two synchronization conditions are of interest. We say the N clocks are *frequency* synchronized to a common frequency $1/T$ if $t_i(n+1) - t_i(n) = T$ for each i and for sufficiently large n . A more strict condition requires full *frequency and phase* synchronization, i.e., $t_1(n) = \dots = t_N(n)$ for n sufficiently large.

Towards the goal of achieving synchronization, clocks are coupled through the transmission by each node, say the i th, of a waveform $g(t)$ at each tick of the local clock $t_i(n)$, either in a given dedicated bandwidth or spread spectrum code or in an overlay system such as UWB (see lower part of fig. 1) [3]. Nodes are assumed to be half-duplex, which implies that, when transmitting, they are not able to receive. Assuming that $g(t)$ is a time-limited pulse, such as a truncated Nyquist waveform, any i th node can then switch from transmit to receive mode (or viceversa) right after (or before) transmission of a pulse at times $t_i(n)$. If $W_g \propto 1/B$ represents the duration of pulse $g(t)$ (with bandwidth B) and W_s is the switching time between transmit and receive modes, the sum $2W = 2W_s + W_g$ represents the refractory time around $t_i(n)$ when the i th node cannot receive (see fig. 2). When receiving, nodes process the combination of pulses received from other nodes with the aim of reaching a synchronized state, as explained below. Notice that, from this discussion, time $2W$ sets a lower bound on the resolution of the synchronization process².

²A way to overcome this limitation could be to use (possibly random) pulse transmission scheduling among the clocks so as to enable the nodes to observe the synchronization signal from other nodes (fig. 2) without refractory times in given periods.

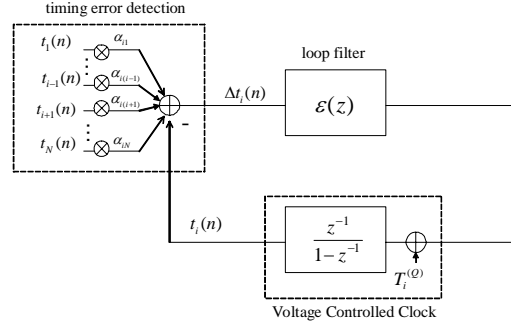


Fig. 3. Equivalent block diagram of a discrete-time PLL with infinite-resolution time error detector, where the delays q_{ij} have been incorporated in the "effective" local frequencies $1/T_i^{(Q)}$.

2.1. Distributed pulse-coupled discrete-time PLLs

In [3] a pulse detector is run at each node on the received signal with the goal of updating the local clock according to the integrate-and-fire mechanism introduced in [11]. Extending the work in [8] [9] [2], here we study an alternative approach based on the familiar mechanism of discrete-time PLLs, that will be shown to have desirable properties in terms of flexible design and relative ease of analysis.

2.1.1. Basic mechanism with ideal time difference detectors

In order to explain the basic idea, let us assume for now that each node, say the i th, is able at each period n to estimate the difference between its own clock $t_i(n)$ and that of other nodes $t_j(n)$ ($j \neq i$) from the received signal sketched in fig. 2, up to the inevitable propagation and processing delay. More precisely, defining as q_{ij} the delay between transmission of pulse $g(t - t_j(n))$ by node j and processing of the latter at node i (by symmetry, we have $q_{ij} = q_{ji}$), node i measures the "delayed" time difference $t_j(n) + q_{ij} - t_i(n)$. What we are neglecting at this stage is the finite time-resolution of the transmitted waveform $g(t)$, the refractory time $2W$ and noise at the receiver side. We discuss these issues in Sec. 2.1.2. However, similarly to [5], we do not assume a fully meshed network where nodes know the time differences with respect to all other nodes. On the contrary, such measurements are possible only between "neighboring" nodes, as detailed below.

Based on the time-difference measurements, the i th clock updates its instantaneous phase $\theta_i(n)$ in $t_i(n) = nT_i + \theta_i(n)$ (see fig. 1). This operation is performed according to a discrete-time PLL (see fig. 3). In particular, a *timing error detector* estimates a convex combination of the "delayed" time differences $t_j(n) + q_{ij} - t_i(n)$ for $j \neq i$, at the n th period. This resembles the operation performed by the phase detector in the system of distributed analog PLLs of [4]. Defining as $\alpha_{ij} \geq 0$ and $\sum_{j=1, j \neq i}^K \alpha_{ij} = 1$ the convex combination weights, we easily get that the output of the time error detector reads $\Delta t_i^{(Q)}(n+1) = \Delta t_i(n+1) + Q_i$, where the convex combination of (non-delayed) time differences is defined as

$$\Delta t_i(n+1) = \sum_{j=1, j \neq i}^N \alpha_{ij} (t_j(n) - t_i(n)) \quad (1)$$

and $Q_i = \sum_{j=1, j \neq i}^N \alpha_{ij} q_{ij}$. The measure $\Delta t_i^{(Q)}(n+1)$ is fed to a loop filter $\varepsilon(z) = \varepsilon_0/(1 - \mu z^{-1})$, where $0 < \varepsilon_0 < 1$ denotes

the loop gain and $0 \leq \mu < 1$ the loop pole. As it customary in the literature on PLLs (see, e.g., [7] [4]), we limit the scope to first ($\mu = 0$) and second ($\mu \neq 0$) - order PLLs. The output of filter $\varepsilon(z)$ drives the local Voltage Control Clock (VCC) as

$$\begin{aligned} t_i(n+1) - t_i(n) &= \varepsilon_0 \Delta t_i^{(Q)}(n+1) + \mu(t_i(n) - t_i(n-1)) \\ &\quad + (1-\mu)T_i \quad (2a) \\ &= \varepsilon_0 \Delta t_i(n+1) + \mu(t_i(n) - t_i(n-1)) \\ &\quad + (1-\mu)T_i^{(Q)}. \quad (2b) \end{aligned}$$

where $T_i^{(Q)} = T_i + \varepsilon_0 Q_i / (1 - \mu)$.

Equation (2) defines the dynamics of the set of pulse-coupled discrete-time PLLs over a connectivity graph defined by weights a_{ij} under the idealistic assumptions of infinite-resolution time error detectors. Notice that the impact of delays has been incorporated in the definition of "effective" free-oscillation periods $T_i^{(Q)}$, so that the PLLs can be described equivalently as in fig. 3. We can conclude that delays have the same effect as frequency offsets of the local clocks. Moreover, we remark that, differently from packet-based schemes, the delays q_{ij} (and thus Q_i) do not depend on the random queuing and processing delays due to creation of packets and medium access control, while depending solely on propagation and processing times at the baseband level. Finally, in order to compensate for delays, each node only needs an estimate of the aggregate measure Q_i , which, in the case of a large number of nodes, might be obtained from ensemble statistics of the network topology.

Convergence analysis of the set of pulse-coupled PLLs (2) (with infinite-resolution time error detectors) is studied in Sec. 3, borrowing some graph algebraic tools from the analysis of consensus algorithms [5].

2.1.2. Finite-resolution time error detectors

In the discussion above, it was assumed that any i th node is able to measure the time differences with respect to neighboring nodes (i.e., nodes j such that $\alpha_{ij} > 0$) so as to calculate the (delayed) time error $\Delta t_i^{(Q)}(n)$. Here we remove this assumption by considering the finite resolution of the transmitted waveform $g(t)$, the refractory time $2W$ due to half-duplex constraint and switching time, and the noise at the receiving side. For the sake of illustration, we present a specific scheme but variants are possible as well. Any i th node, at the n th period, observes the received signal $y_i(n, t)$ over a time window of size equal to the local period T_i around the firing instant $t_i(n)$, with the exception of the time interval of duration $2W$ around $t_i(n)$ because of the half-duplex constraint (see fig. 2 for a sketch with arbitrary waveforms and no noise). The transmitted pulse $g(t)$ is a truncated square-root Nyquist waveform with roll-off δ , such that the autocorrelation $r_g(t)$ has peak-to-first zero time $W_p = (1 + \delta)/(2B)$ (a reasonable figure is $W_g = 6W_p$). The i th node performs baseband filtering matched to the transmitted waveform $g(t)$, and then samples the received signal at some multiple L of the symbol frequency $1/W_p$, i.e., L/W_p with $L \geq 1$. This operation produces the samples $y_i(n, m)$ in the n th observation window, where $m \in \mathcal{J} = \{(-0.5LT_i/W_p, \dots, -[LW/W_p]) \cup ([LW/W_p], \dots, 0.5LT_i/W_p)\}$, the sample $m = 0$ corresponding to the "firing" instant $t_i(n)$ (recall fig. 2):

$$y_i(n, m) = \sum_{j=1, j \neq i}^N \sqrt{E_{ij}} \cdot r_g \left(\frac{mW_p}{L} - (t_j(n) + q_{ij} - t_i(n)) \right) + w(n, m).$$

In (3), the waveform r_g is the autocorrelation of $g(t)$, the average energy per symbol reads $E_{ij} = P_{ij}W_g$ (assuming $r_g(0) = 1$), and $w(n, m)$ is the additive Gaussian noise with zero mean and power N_0 .

Based on the samples $y_i(n, m)$, the time error detector at i th node needs to estimate the quantity $\Delta t_i^{(Q)}(n) = \sum_{j=1, j \neq i}^N \alpha_{ij} (t_j(n) + q_{ij} - t_i(n))$. Inspired by [9], here we propose an effective time detector that *does not need to explicitly estimate the arrival times* $t_j(n) + q_{ij}$ ($j \neq i$). To illustrate the idea, consider the specific choice for the convex weights α_{ij}

$$\alpha_{ij} = \frac{P_{ij}}{\sum_{j=1, j \neq i}^N P_{ij}}, \quad (4)$$

as proposed in [8] and [9] for first-order discrete-time PLLs. According to (4), the ideal time error detector evaluates the weighted average of the time differences $t_j(n) + q_{ij} - t_i(n)$ based on the fraction of power received on the corresponding pulse. A possible estimate of $\Delta t_i^{(Q)}(n)$ can then be obtained as the following "center-of-mass" timing detector:

$$\widehat{\Delta t}_i^{(Q)}(n) = \sum_{j \in \mathcal{J}} \hat{\alpha}_{ij} \cdot \frac{jW_p}{L} \quad (5a)$$

$$\hat{\alpha}_{ij} = \frac{|y_i(n, j)|^2}{\sum_{k \in \mathcal{J}} |y_i(n, k)|^2}. \quad (5b)$$

With the simple implementation of the time error detector described in (5), all the received samples are weighted by the instantaneous received power in order to evaluate the "center of mass" of the received signal in order to drive the voltage controlled clock (2a). Possible variants include the introduction of a threshold on the received power in order to include only a subset of significant times in the sum (4) (see [9]). The performance of this scheme will be investigated in Sec. 4 via numerical results.

3. SYSTEM ANALYSIS

In this section, we analyze the convergence properties of the system of pulse-coupled PLLs under the idealistic assumption of infinite resolution time error detector. Under this condition, equation (2b) holds and the dynamics of the system can be easily shown to be described by the first-order vector difference equation

$$\mathbf{t}(n+1) = (\mathbf{A} + \mu \mathbf{I}) \cdot \mathbf{t}(n) - \mu \mathbf{t}(n-1) + (1-\mu)\mathbf{T}, \quad (6)$$

where we defined the vectors $\mathbf{t}(n) = [t_1(n) \dots t_N(n)]^T$ and $\mathbf{T} = [T_1^{(Q)} \dots T_N^{(Q)}]^T$. Moreover, the system matrix reads $\mathbf{A} = \mathbf{I} - \varepsilon_0 \mathbf{L}$, with \mathbf{L} being the graph Laplacian of the network: $[\mathbf{L}]_{ii} = \sum_{j \neq i} \alpha_{ij} = 1$ (i.e., the degree of node i) and $[\mathbf{L}]_{ij} = -\alpha_{ij}$ for $i \neq j$. Notice that matrix \mathbf{A} is stochastic: $\mathbf{A} \cdot \mathbf{1} = \mathbf{1}$. Model (6) coincides with the framework considered in the literature on consensus of multi-agent networks for the special case $\mu = 0$ and $\mathbf{T} = \mathbf{0}$ [5]. In other words, the consensus model describes a scenario with first-order PLLs ($\mu = 0$) and frequency synchronous clocks ($\mathbf{T} = \mathbf{0}$). Therefore, from the results surveyed in [5], we can readily conclude that, with $\mu = 0$ and frequency synchronous clocks, if the connectivity graph of the network is strongly connected (or equivalently matrix \mathbf{A} is irreducible), system (6) achieves full synchronization (with an exponential rate).

We now focus on the general case of $\mu > 0$ and frequency asynchronous clocks (i.e., $T_i \neq T_j$ for $i \neq j$). Let us denote a possible

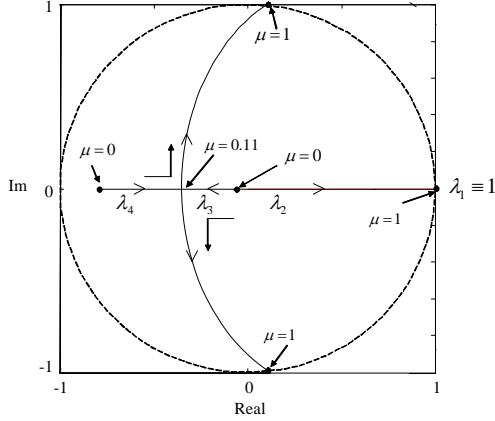


Fig. 4. Eigenvalues of the second order loop system (6) (i.e., of matrix (11)) in the case of two users with μ increasing from 0 to 1 ($\varepsilon_0 = 0.9$).

value for the synchronized frequency as $1/T$ (to be determined), i.e., $t_i(n) - t_i(n-1) = T$ for sufficiently large n , so that the clock of the i th node can be written (for large n) as

$$t_i(n) = nT + \tau_i(n), \quad (7)$$

where $\tau_i(n)$ denotes the relative phase with respect to the common frequency. In vector form, the previous equation becomes $\mathbf{t}(n) = nT \cdot \mathbf{1} + \boldsymbol{\tau}(n)$ with $\boldsymbol{\tau}(n) = [\tau_1(n) \cdots \tau_N(n)]^T$. The equilibrium point (steady state) of the system (6) is identified by the following proposition.

Proposition 1: If the network of distributed PLL is strictly connected, the equilibrium point of system (6) is characterized by solutions $\mathbf{t}(n) = nT \cdot \mathbf{1} + \boldsymbol{\tau}^*$, where the common period reads

$$T = \mathbf{v}^T \mathbf{T}, \quad (8)$$

with \mathbf{v} being the normalized left eigenvector of matrix \mathbf{A} corresponding to eigenvalue 1 ($\mathbf{A}^T \mathbf{v} = \mathbf{v}$ with $\mathbf{1}^T \mathbf{v} = 1$), and the steady-state phase vector $\boldsymbol{\tau}^*$ is

$$\boldsymbol{\tau}^* = \mathbf{1} \cdot \eta + (1 - \mu) \frac{\mathbf{L}^\dagger}{\varepsilon} \boldsymbol{\Delta} \mathbf{T}, \quad (9)$$

with $(\cdot)^\dagger$ denoting the pseudoinverse, and with definitions

$$\eta = \mathbf{v}^T \left(\boldsymbol{\tau}(0) - (1 - \mu) \frac{\mathbf{L}^\dagger}{\varepsilon} \boldsymbol{\Delta} \mathbf{T} \right) \quad (10)$$

and $[\boldsymbol{\Delta} \mathbf{T}]_k = T_k - T$.

Proof: see Appendix.

Proposition 1 is the counterpart of known facts in the analysis of conventional PLLs, wherein first and second order loops lead to a static phase error that is proportional to the frequency mismatch similarly to (9) [7]. It can be seen that introducing a pole μ in the loop causes a reduction in the steady state phase error by a factor $1 - \mu$.

However, it remains to be proved that the system of distributed PLLs actually converges to the steady-state illustrated by Proposition 1. It is pretty straightforward, by using the results surveyed in [5], to

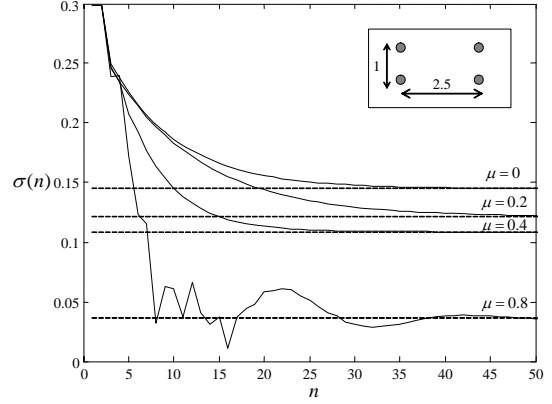


Fig. 5. Standard deviation of the clocks $\{t_i(n)\}_{i=1}^N$ versus period index n : infinite resolution. Dashed lines correspond to the analytical result (9).

prove that convergence is guaranteed for any $0 < \varepsilon_0 < 1$ if $\mu = 0$ (first-order PLLs). However, the same is not true for second-order PLLs ($0 < \mu < 1$). Referring to [10] for further analysis on this point, here we illustrate the issue by means of an example. Consider a network with two nodes. In this case, we have $\alpha_{12} = \alpha_{21} = 1$ and the graph is connected. Fig. 4 shows the four eigenvalues of the system matrix associated with (6)

$$\tilde{\mathbf{A}} = \begin{bmatrix} \mathbf{A} + \mu \mathbf{I} & -\mu \mathbf{I} \\ \mathbf{I} & \mathbf{0} \end{bmatrix}, \quad (11)$$

for different values of the pole μ and $\varepsilon_0 = 0.9$. Notice that the system matrix (11) is 4×4 since (6) is a system of two second order difference equations. Moreover, one eigenvalue of $\tilde{\mathbf{A}}$ is 1 irrespective of the value of μ . The absolute value of the remaining eigenvalues tends to one for $\mu \rightarrow 1$, showing that increasing the value of the pole in the loop filter $\varepsilon(z)$ leads to lack of stability of the equilibrium point (9). It can be concluded that, as in the case of conventional PLLs [7], the static phase error reduction achieved with the introduction of a pole μ comes at the expense of decreased margins of stability.

4. NUMERICAL RESULTS

In this section, we first corroborate the analysis of infinite-resolution PLLs carried out in the previous section, and then compare this ideal performance with the case of finite resolution studied in Sec. 2.1.2. Let us consider the choice (4) for the weighting coefficients α_{ij} , and a simple geometry with $K = 4$ nodes located on the vertices of a rectangle with side ratio 1:2.5 (see box in fig. 5). Moreover, let us set $C_{ij} = C$ so that the coefficients α_{ij} (4) only depend on relative distances. Fig. 5 shows the standard deviation $\sigma(n)$ of the timing vector $\mathbf{t}(n)$ versus n , where $\sigma^2(n) = 1/4 \cdot \sum_{k=1}^4 (t_k(n) - 1/4 \sum_{k=1}^4 t_k(n))^2$, for $T = 1$, $\boldsymbol{\Delta} \mathbf{T} = [-0.02 \ -0.01 \ 0.01 \ 0.02]^T$ and initial phases $\boldsymbol{\theta}(0) = \boldsymbol{\tau}(0) = [0.1 \ 0.4 \ 0.6 \ 0.8]^T$. Other parameters are selected as $\gamma = 3$ and $\varepsilon_0 = 0.6$. Different values of the pole μ are considered showing: (i) a reduction in steady state synchronization error with increasing μ (dashed lines correspond to the analytical result (9)); (ii) the occurrence of an oscillating behavior

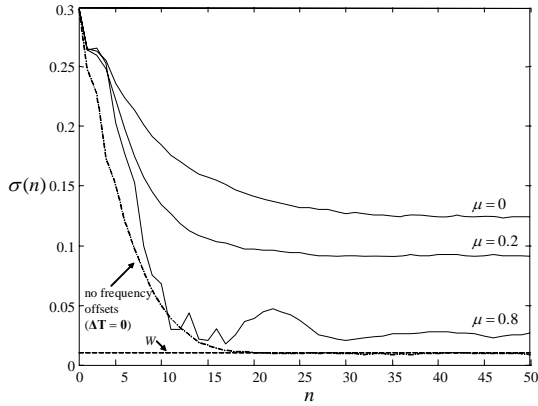


Fig. 6. Standard deviation of the clocks $\{t_i(n)\}_{i=1}^N$ versus period index n : finite resolution.

for increasing μ that leads to lack of convergence for $\mu \rightarrow 1$ (not shown for clarity).

Fig. 6 revisits the previous examples by considering finite resolution, as discussed in Sec. 2.1.2. Roll-off of the waveform $g(t)$ is $\delta = 0.2$, the signal to noise ratio reads $\bar{P}/N_0 = 25\text{dB}$ where \bar{P} is the power received along the short sides of the rectangular topology. Fig. 6 shows the standard deviation $\sigma(n)$ averaged over noise through Monte Carlo simulations. The normalized timing resolution is $W_p = 0.01$, the switching time is set to $W = W_p$ for simplicity and the oversampling factor to $L = 2$. It is seen that the same qualitative behavior of fig. 5 is reproduced by increasing the pole μ even in the case of a practical timing error detector. As a reference, the case with no frequency mismatch $\Delta\mathbf{T} = \mathbf{0}$ is considered. It can be seen that in this case the error floor is set by the half duplex constraint $W = 0.01$.

5. CONCLUSIONS

This paper has investigated pulse-coupled discrete-time PLLs for mutual time synchronization in wireless networks. Propagation delays and finite pulse resolution have been accounted for, and convergence analysis has been provided under simplified assumptions, showing that known results in the context of conventional PLLs for carrier acquisition extend naturally to distributed PLLs.

6. APPENDIX: PROOF OF PROPOSITION 1

The system (6) can be written in terms of phases $\tau(n)$ relative to the common period T as

$$\tau(n+1) - \tau(n) = -\varepsilon_0 \mathbf{L}\tau(n) + \mu(\tau(n) - \tau(n-1)) + (1-\mu)\Delta\mathbf{T}. \quad (12)$$

An equilibrium state τ^* for the difference equation (12) satisfies $\tau(n+1) = \tau(n) = \tau(n-1) = \tau^*$, which yields the condition

$$\mathbf{L}\tau^* = (1-\mu)\frac{\Delta\mathbf{T}}{\varepsilon_0}. \quad (13)$$

From (13), it follows that: (i) in order for (13) to be feasible (i.e., for an equilibrium point to exist), the common clock period T must satisfy $\mathbf{v}^T \Delta\mathbf{T} = \mathbf{0}$ or equivalently (8); (ii) an equilibrium phase vector

τ^* must read $\tau^* = (1-\mu)\frac{\mathbf{L}^\dagger \Delta\mathbf{T}}{\varepsilon} + \eta\mathbf{1}$ where η is an arbitrary constant.

Let us define $\tau'(n) = \tau(n) - (1-\mu)\frac{\mathbf{L}^\dagger \Delta\mathbf{T}}{\varepsilon}$. With this change of variables, the difference equation (12) boils down to

$$\tau'(n+1) = \mathbf{A} \cdot \tau'(n) + \mu(\tau'(n) - \tau'(n-1)). \quad (14)$$

The system (14) is a second-order vector difference equation, that can be studied by recasting it as a first-order vector difference equation in terms of vector $\tilde{\tau}(n) = [\tau'(n)^T \ \tau'(n-1)^T]^T$ with system matrix $\tilde{\mathbf{A}}$ (11). Convergence of the corresponding system $\tilde{\tau}(n) = \tilde{\mathbf{A}}\tilde{\tau}(n-1)$ depends on the eigenvalues of $\tilde{\mathbf{A}}$. It is easy to see that $\tilde{\mathbf{A}}$ has an eigenvalue equal to one, with left and (normalized) right eigenvectors $\mathbf{z}_\ell = \mathbf{1}$ and $\mathbf{z}_r = 1/(1-\mu) \cdot [\mathbf{v}^T \ -\mu\mathbf{v}^T]^T$ (recall that \mathbf{v} is the right eigenvector of \mathbf{A} corresponding to the eigenvalue $\lambda = 1$). Moreover, it can be shown that this eigenvalue is unique [10]. Therefore, the system (14) is stable if and only if all the remaining $2K-1$ eigenvalues of $\tilde{\mathbf{A}}$ have absolute value less than one (see, e.g., [5]). Assuming that the stability condition mentioned above holds, then we have $\tilde{\mathbf{A}}^n \rightarrow \mathbf{z}_\ell \mathbf{z}_r^T$ for $n \rightarrow \infty$ (see, e.g., [5]) and the phases $\tau'(n)$ converge as $\tau'(n) \rightarrow \mathbf{1}\mathbf{v}^T \tau'(0)$ (having set $\tau(-1) = \tau(0)$), which implies that the constant η in (9) is (10).

7. REFERENCES

- [1] F. Sivrikaya and B. F. Yener, "Time synchronization in sensor networks: a survey," *IEEE Network*, vol. 18, no. 4, pp. 45-50, July-Aug. 2004.
- [2] Qun Li and D. Rus, "Global clock synchronization in sensor networks," *IEEE Trans. Computers*, vol. 55, no. 2, pp. 214-226, Feb. 2006.
- [3] Y.-W. Hong, A. Scaglione, "A scalable synchronization protocol for large scale sensor networks and its applications," *IEEE Journal Selected Areas Commun.*, vol. 23, no. 5, pp. 1085-1099, May 2005.
- [4] W. C. Lindsey, F. Ghazvinian, W. C. Hagmann and K. Deseouky, "Network synchronization," *Proc. of the IEEE*, vol. 73, no. 10, pp. 1445-1467, Oct. 1985.
- [5] Wei Ren, R. W. Beard and E. M. Atkins, "A survey of consensus problems in multi-agent coordination," in *Proc. American Control Conference*, vol. 3, pp. 1859-1864, June 2005.
- [6] G. Scutari, S. Barbarossa and L. Pescosolido, "Optimal decentralized estimation through self-synchronizing networks in the presence of propagation delays," in *Proc. SPAWC 2006*.
- [7] F. M. Gardner, *Phaselock Techniques*, John Wiley & Sons, Inc., 1966.
- [8] F. Tong and Y. Akaiwa, "Theoretical analysis of interbase-station synchronization systems," *IEEE Trans. Commun.*, vol. 46, no. 5, pp. 590-594, 1998.
- [9] E. Sourour and M. Nakagawa, "Mutual decentralized synchronization for intervehicle communications," *IEEE Trans. Veh. Technol.*, vol. 48, no. 6, pp. 2015-2027, Nov. 1999.
- [10] O. Simeone and U. Spagnolini, "Distributed time synchronization in wireless sensor networks with coupled discrete-time oscillators," submitted to *Eurasip Journ. on Wireless Commun. and Networking* (invited).
- [11] R. E. Mirollo and S. H. Strogatz, "Synchronization of pulse-coupled biological oscillators," *SIAM Journal on Applied Mathematics*, vol. 50, no. 6, pp. 1645-1662, Dec. 1990.